JOURNAL OF GUIDANCE, CONTROL, AND DYNAMICS
Vol. 24, No. 6, November–December 2001

Using a Multiple-Model Adaptive Estimator in a Random Evasion Missile/Aircraft Encounter

Y. Oshman* and J. Shinar†
Technion–Israel Institute of Technology, Haifa 32000, Israel
and
S. Avrashi Weizman‡
RAFAEL, Ministry of Defense, Haifa 31021, Israel

The terminal phase (end game) of an encounter between an air-to-air missile equipped with an active monopulse radar seeker and an evading fighter aircraft, possibly employing electronic countermeasures in the form of electronic jinking, is addressed. The missile uses a guidance law derived from linear differential game theory, which is implemented by using a multiple-model adaptive estimator (MMAE). The MMAE identifies the evasion strategy of the aircraft, which consists of the combination of evasion maneuver and electronic jinking. An extensive numerical study is used to demonstrate the viability of the concept. In comparison with a previously proposed mixed strategy guidance methodology, the new MMAE-based approach leads to a substantial improvement in the guaranteed single-shot kill probability for the missile.

I. Introduction

MODERN air-to-air missiles, designed to intercept highly maneuverable aircraft equipped with electronic countermeasures (ECM), have to operate in a highly uncertain environment. This paper is concerned with the terminal phase (end game) of an encounter between a missile equipped with an active monopulse radar seeker and an evading fighter aircraft having the option to use ECM. The terminal homing phase of the interception starts when the active seeker of the missile locks on its target, generating also a warning signal (including some threat identification) in the aircraft. This warning is the only information the pilot has. At the moment when the warning is received, the pilot starts to execute a sequence of periodical evasive maneuvers. Simultaneously, to enhance its survivability, the pilot may also switch on the aircraft's ECM system, which produces electronic jinking (EJ), a periodic switching of the aircraft's apparent radar reflection center from one wingtip to the other.[1] The respective frequencies of the evasive maneuver (EM) and the EJ are assumed to be independent. The evasion strategy of the aircraft, comprising the pair {EM, EJ}, is unknown to the missile's homing system.

Earlier studies investigating such a scenario[2–5] showed that the combination of periodical aircraft maneuvers and EJ, both of unknown frequency and random phase, has a devastating effect on the homing accuracy of any guided missile using classical guidance laws, namely, proportional navigation (PN) and augmented PN, implemented using a single, simple, fixed-gain (nonadaptive) estimator. For this reason, Refs. 2–5 used a nonlinear guidance law that was developed based on a perfect information linear differential game model with bounded control.[6,7] This guidance law [called in the sequel differential game law (DGL)] requires the knowledge of the line of sight (LOS) rate (similarly to PN) and also incorporates a compensation term for the missile's own dynamic delay, but does not require information on the actual target maneuver. If the assumption of perfect information is valid, this guidance law guarantees a very small, but nonzero, miss distance if the missile/target maneuverability ratio is sufficiently high (about three or higher). It was demonstrated [3,8] that DGL is much more robust with respect to target maneuver estimation error than guidance laws based on an optimal control approach.[9]

The application of DGL in a missile with a radar seeker (of inherently noisy measurements) requires the use of an estimator to obtain the best estimate of the LOS rate. It has been of common practice in the missile community to design the guidance law and the estimator independently. Although this guidance law itself does not require the explicit knowledge of the target maneuver, for the estimator design some implicit assumptions on the target motion (including its lateral acceleration) are also necessary. If the assumption on the target behavior is correct, the estimated LOS rate will be accurate, and the interception will result in a very small miss distance. However, a wrong assumption on the target maneuver yields a bad estimate of the LOS rate and, as a consequence, large miss distances. One of the first conclusions of the earlier studies[2,3] was that it is impossible to find a single estimator that is capable of providing satisfactory homing performance for the entire expected spectrum of periodic aircraft maneuvers and EJ. To alleviate this difficulty, a mixed strategy approach was proposed.[2,4] According to this approach, several fixed-gain estimators are included in the missile's homing system, each covering a part of the expected scenario spectrum. At the beginning of the end game, one of them is selected randomly to provide the LOS rate information to the guidance law. The rationale behind this approach is the concern that the short duration of the end game precludes the identification of the actual evasive strategy of the target. Therefore, random guess is the best possible option. The results of the mixed strategy approach showed an important improvement compared to pure strategy (single estimator) designs. However, it was also found[5] that identification of the existence of eventual EJ in real time can provide an even better homing performance.

State estimators, designed to provide the missile guidance law with the best target state estimate in spite of all elements of uncertainty, have been incorporated in maneuvering target tracking systems for the last three decades.[10] In most common mathematical formulations of the target tracking problem, the associated estimation problem is highly nonlinear. The application of some nonlinear filtering technique is, therefore, almost inevitable. To date, the majority of estimation methods used in practice have been based on the widely accepted extended Kalman filtering (EKF) approach. Because the time-varying maneuvering target acceleration cannot be measured, and its statistics cannot be exactly known, some assumptions must be made about the target behavior. The mathematical modeling of the target acceleration constitutes a critical factor in the design of the estimator. As is well known, the basic EKF is

Presented as Paper 99-4141 at the AIAA Guidance, Navigation, and Control Conference, Portland, OR, 9–11 August 1999; received 14 April 2000; revision received 16 January 2001; accepted for publication 9 February 2001.

*Associate Professor, Department of Aerospace Engineering; Yaakov.Oshman@technion.ac.il. Associate Fellow AIAA.

†Max and Lottie Dresher Professor of Aerospace Performance and Propulsion, Department of Aerospace Engineering. Fellow AIAA.

‡Research Engineer, P.O. Box 2250, Armament Development Authority.

very sensitive to modeling errors, which might result in poor filter performance, leading to unacceptable miss distances.

Various acceleration models have been proposed over the years, differing in their level of complexity.[11,12] Detection algorithms, which discriminate between different hypotheses on the target maneuvering state based on the filter residuals, have been used to extend the performance of the basic EKF algorithm.[13] However, these algorithms generally suffer from detection delays, poor transient tracking performance after detection, and degraded performance in the presence of smooth target acceleration.

Multiple-model adaptive estimation (MMAE) methods[14] have long been used in a wide range of applications. Common to all of these methods is the use of a set (bank) of model-matched parallel estimators and a fusion algorithm, commonly based on either the minimum mean square error estimation or the maximum a posteriori (MAP) criterion. The major advantage of the MMAE approach is that it allows for the explicit inclusion of all target maneuver modes in the mathematical formulation of the estimation problem, through the use of a finite number of different models, each corresponding to a different maneuver mode. Existing MMAE methods can be classified as belonging to the one of the following classes: 1) static methods, in which the true system behavior is assumed to be time invariant, that is, one of the models in the bank is assumed to be matched to the true system, and 2) dynamic methods, which allow for a time-varying system behavior by including a mechanism for switching between system modes according to a prescribed transition probability matrix. In all MMAE methods, the computational burden associated with the number of filters in the bank is a major implementation concern, and various methods have been suggested to alleviate this problem.

Recent advances in microprocessor technology make it feasible to develop complex, yet realizable estimation algorithms. Based on this observation, the present study is aimed at assessing the feasibility of implementing a relatively powerful yet practical estimator as a means of improving the terminal homing performance of a DGL-guided air-to-air missile with a radar seeker against an agile evading aircraft equipped with an ECM system. As mentioned, it was shown[5] that real-time identification of the aircraft evading strategy (in particular, the very existence of an active ECM mode and the identification of this mode) can greatly enhance the performance of a DGL-guided missile. Making the reasonable assumption that the target strategy remains constant during the short duration of the end game (typically a few seconds), a static, reduced-order MMAE was implemented that identifies the strategy elements of the target, that is, the existence and the respective frequencies of the maneuvering acceleration and of the EJ. The homing performance of this innovative guidance approach was tested using a very large number of Monte Carlo simulations. To the best of the authors' knowledge, such analysis of an air-to-air interception scenario has not been carried out before.

The remainder of this paper is organized as follows. In the next section the end game problem under consideration is mathematically formulated. This includes the description of the interception scenario, definition of the target's evasion strategy elements, and the missile guidance law. The implementation of the MMAE and its tailoring to the problem at hand is described in Sec. III. An extensive simulation study, which was performed to assess the merits of the proposed approach, is presented and discussed in Sec. IV. Concluding remarks are offered in the final section.

II. Problem Formulation

A. Dynamic Model

The air-to air interception scenario described in the Introduction takes place at a constant altitude in a head-on geometry, which provides the shortest end game with the highest closing speed. It is assumed that both the air-to-air missile and the target aircraft fly at a constant velocity. After being alerted by the warning that the active radar seeker is locked-on, the target aircraft starts a sequence of evasive hard horizontal turns, combined with the eventual application of EJ. Because the turning maneuvers are executed by appropriate rolling of the aircraft, the wingtips of the aircraft, where the reflection sources of the EJ are installed, are not in the same horizontal plane as the aircraft's center of gravity, as shown in Fig. 1. Thus, the mathematical model for simulating the end game must be three dimensional.

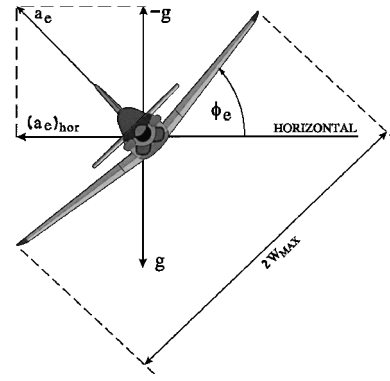

Fig. 1 Forward view of a maneuvering aircraft.

1. *Equations of Relative Motion*

To formulate the equations of relative motion between the target and the missile, the following coordinate systems will be used. Let $\mathcal{S}_p$ and $\mathcal{S}_e$ denote Cartesian coordinate systems attached to the missile and target bodies, respectively. Correspondingly, let the axes in these coordinate systems be denoted by (X_p, Y_p, Z_p) and (X_e, Y_e, Z_e), respectively. The reference coordinate system $\mathcal{S}_i$, in which the equations of motion will be formulated in the sequel, is a nonrotating Cartesian system, whose origin is affixed to the missile center of gravity with axes X_i along the initial LOS, Z_i in the vertical plane pointing downward, and Y_i in the horizontal plane, complementing the first two axes according to the right-hand rule.

Let the angular attitudes of $\mathcal{S}_p$ and of $\mathcal{S}_e$ relative to the nonrotating frame of reference $\mathcal{S}_i$ be represented by the Euler angle triads $(\psi_p, \theta_p, \phi_p)$ and $(\psi_e, \theta_e, \phi_e)$, respectively, where the rotation sequence in both frames of reference is 3–2–1. The target's location relative to the missile is defined by y and z, which denote the Y_p and Z_p components, respectively, of the target's center of gravity location in the missile frame of reference.

Written in the nonrotating reference frame $\mathcal{S}_i$, the equations of relative motion between the target and the missile become

$$\dot{x} = v_e \cos\psi_e - v_p \cos\psi_p \cos\theta_p \tag{1a}$$

$$\dot{y} = v_e \sin\psi_e - v_p \sin\psi_p \cos\theta_p \tag{1b}$$

$$\dot{z} = v_p \sin\theta_p \tag{1c}$$

where v_p and v_e are the missile and target velocities, respectively.

2. *Target EM*

The absolute value of the lateral acceleration of the aircraft, related to its bank angle ϕ_e by

$$a_e = g/\cos\phi_e \tag{2}$$

is limited by the maximal allowable load factor $a_{e\max} = gn_{\max}$. Thus, the maximal absolute value of the bank angle is given by

$$\phi_{e\max} = \cos^{-1}\left(g/a_{e\max}\right) \tag{3}$$

The rate of change of the bank angle is limited by the maximum permissible roll rate of the aircraft, characterized by t_r, the time required to roll the aircraft by a bank angle of $2\phi_{e\max}$, as shown in Fig. 2. An aircraft EM may consist of either 1) a constant maneuver characterized by $\phi_{e\max}$ or 2) a periodic maneuver with random phase, where the roll angle is given by

$$\phi_e(t) = \phi_{e\max}\,\mathrm{sat}\left[\phi_e^u(t)\right] \tag{4}$$

where

$$\phi_e^u(t) = \begin{cases} \omega_m t + \psi_m & 0 \le \omega_m t \le \pi/2 - \psi_m \\ -\omega_m t - \psi_m + \pi & \pi/2 - \psi_m \le \omega_m t \le 3\pi/2 - \psi_m \\ \omega_m t + \psi_m - 2\pi & 3\pi/2 - \psi_m \le \omega_m t \le 5\pi/2 - \psi_m \end{cases}$$

$$\phi_e^u(t + 2\pi/\omega_m) = \phi_e^u(t) \tag{5}$$

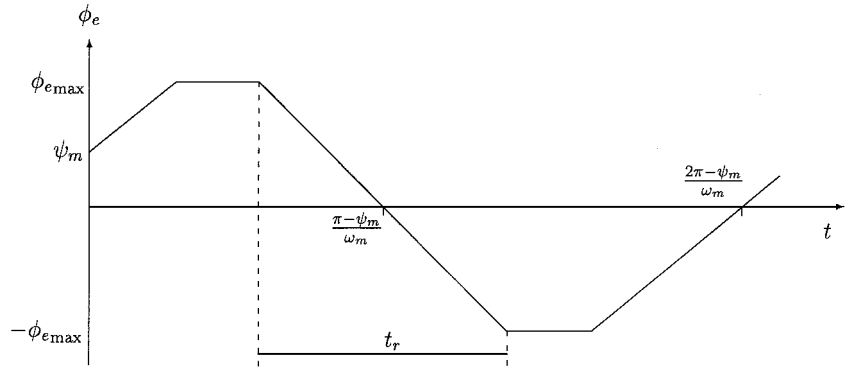

Fig. 2 Roll angle vs time.

where ω_m is the frequency of the periodic maneuver and ψ_m is the random phase. A typical time history of the target's roll angle is shown in Fig. 2.

3. Missile Guidance Law

The interceptor missile is represented by a point-mass model (three degrees of translational freedom). It is assumed to be roll stabilized and has two identical guidance channels operating in the horizontal and the vertical plane. It has first-order control dynamics with time constant τ_p. Therefore, the relationship between the actual lateral acceleration a_p and its command a_c is given in both channels by

$$\dot{a}_p = (a_c - a_p)/\tau_p \tag{6}$$

The guidance law of the missile is DGL.[6] It is based on computing (or estimating) in each guidance channel the component of the zero-effort miss distance (ZEM), that is, the miss distance that would be obtained without any further acceleration command and no target maneuver

$$\mathrm{ZEM}_\xi = \xi + t_{\mathrm{go}}\dot{\xi} - \tau_p^2(e^{-T} + T - 1)a_{p\xi}, \qquad \xi = y, z \tag{7}$$

where $t_{\mathrm{go}} = t_f - t$ is the time to go and t_f is the time at the end of the end game. The lateral acceleration command in each channel is given by the following two-stage model:

1) In the first stage, the guidance command in each channel is linear in ZEM and is given by

$$a_c = \left(N'/t_{\mathrm{go}}^2\right)\mathrm{ZEM} \tag{8}$$

where

$$N' = 2/[(1 - 1/\mu) - 2(e^{-T} + T - 1)/T^2] \tag{9}$$

where $\mu = a_{p\max}/a_{e\max}$ is the missile/target maximal acceleration ratio and $T = t_{\mathrm{go}}/\tau_p$.

2) In the second stage, the guidance law is of a bang–bang type

$$a_c = a_{p\max}\,\mathrm{sgn}(\mathrm{ZEM}) \tag{10}$$

The guidance law switches from the first to the second stage at $T = T_s$, where T_s is the normalized time to go for which the denominator in Eq. (9) vanishes. In addition, a dead zone (DZ) was introduced in the final stage. The two-stage guidance law thus becomes

$$a_c = \begin{cases} a_{p\max}\,\mathrm{sat}\left\{\dfrac{N'}{t_{\mathrm{go}}^2}\dfrac{\mathrm{ZEM}}{a_{p\max}}\right\} & T > T_s \\ a_{p\max}\,\mathrm{sgn}(\mathrm{ZEM}) & T \le T_s, \quad |\mathrm{ZEM}| > \mathrm{DZ} \\ 0 & T \le T_s, \quad |\mathrm{ZEM}| \le \mathrm{DZ} \end{cases} \tag{11}$$

4. Information Structure

The engagement is formulated as a zero-sum pursuit evasion game of fixed duration with imperfect information. As mentioned in the Introduction, the only information the aircraft (the evader) has is that the engagement has started, but no information is available on the relative position of the interceptor missile (the pursuer). The missile is assumed to have an ideal seeker that measures the relative position (range, range rate, and direction) of the evader, but these measurements are corrupted by noise and affected by the EJ.

The noise model assumed in this study concentrates on glint, which has the major effect in the end game. Glint is a random motion of the target's center of radar reflection due to a complex interaction between its different parts. It is usually characterized as a Gaussian, zero-mean random process with bandwidth on the order of 1–2.5 Hz and standard deviation from about one-fifth to one-half of the aircraft half-wingspan. In the simulation program of this study, the glint noise was modeled as the output of a bandpass linear filter driven by white noise. Because the reflected signal due to EJ is much stronger than the natural radar reflection of the aircraft's skin, when EJ is active the glint noise is negligible.

It is assumed that the range and range rate are obtained with a relatively good accuracy. Therefore, the time to go, required for implementing the guidance law, is available. Only the measurements of the LOS direction are affected by the noise and the EJ. The missile's own acceleration is also accurately measured. With these measurements, the missile estimates the components of the ZEM in each channel based on Eq. (7). The measured input to each guidance channel includes the position of the target normal to the LOS, corrupted by glint noise and/or w_j, the respective component of the EJ given by

$$w_j = W_{\max}\,\mathrm{sgn}[\cos(\omega_j t + \psi_j)] \tag{12}$$

In this equation, $W_{\max}$ is half of the wingspan of the aircraft, ω_j is the EJ frequency, and ψ_j is a random phase.

B. Evasion Strategy Set

Although the possible combinations of periodical maneuvers and EJ are infinite, it was decided, as in similar previous works,[2–5] to limit the study to a finite set of evasion strategies that represents the feasible domain of maneuvers to be used with various ECM options. The evasion strategy set in this study is composed of 45 elements, each being a combination of a maneuvering option and an EJ option. The nine maneuvering options are no maneuver, (NM), constant maneuver (CM) ($\omega_m = 0$), and random phase periodic maneuver (EM) at the frequencies $\omega_m = 0.25$, 0.5, 0.75, 1.0, 1.5, 2.0, and 3.0 rad/s. The five EJ options are no EJ (NJ), constant EJ (CJ) ($\omega_j = 0$), and random phase periodic EJ at the frequencies $\omega_j = 1.0$, 2.0, and 3.0 rad/s.

C. Lethality Model

A realistic lethality model of a missile's warhead against an evading aircraft is very complex. It depends on many physical parameters as well as on an accurate (six degrees of freedom) terminal geometry. In the simplified point-mass model, assumed herein, the only

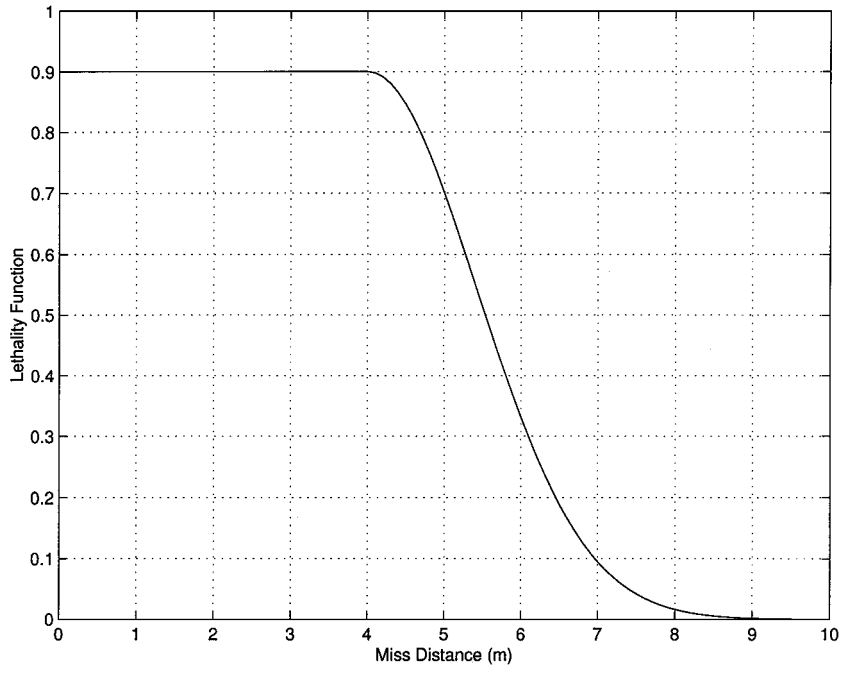

Fig. 3 Lethality function.

available information is R_f, the miss distance measured between the respective centers of gravity. It is assumed that the warhead detonates at the point of closest approach (the very definition of the miss distance) and that the target's vulnerability is uniform. In this study the probability of destroying the target is determined by the following single valued (lethality) function of the miss distance, which expresses how the warhead efficiency smoothly and rapidly decays beyond a characteristic radius R_k

$$P_d(R_f) = \begin{cases} P_{d\max} \exp\left[-4(R_f/R_k - 1)^2\right] & R_f > R_k \\ P_{d\max} & R_f \le R_k \end{cases} \tag{13}$$

where $P_{d\max}$ is the overall reliability of the entire guidance system and R_k is the characteristic lethal (kill) radius of the warhead. This lethality function is depicted in Fig. 3 for the parameters $P_{d\max} = 0.9$ and $R_k = 4$ m, used in this study.

D. Performance Measure

The real cost function in a perfect information interception scenario is the miss distance, to be maximized by the evading aircraft and minimized by the guided missile. This miss distance is associated by the lethality model (13) with the probability of target destruction. In the imperfect information scenario of this study, the miss distance and the associated probability of target destruction become random variables in any given realization of an evasion strategy of the aircraft. Taking the mathematical expectation of the kill probability over the entire set of possible realizations of the evasion strategy space provides the single-shot kill probability (SSKP) of the missile against this particular evasion strategy

$$\text{SSKP} = E\{P_d(R_f)\} \tag{14}$$

If the SSKP values are known for each admissible evasion strategy, the aircraft can select that strategy that is associated with the lowest SSKP. However, the kill probability also depends on the missile parameters and its guidance system, comprising the estimator and the guidance law. By the use of the MMAE technique described in the next section, this study aims at maximizing the minimal value of the SSKP over the entire set of admissible evading strategies. This minimal value is called the guaranteed SSKP of the interception. From a game theoretical point of view, the guaranteed SSKP is the value of the game with imperfect information.

III. Estimator Design

A. MMAE Theory

In this section we briefly review the fundamental principles of MMAE theory. Full mathematical development can be found in Ref. 14. MMAE is a method of estimating unknown system parameters by modeling different parameter values in several Kalman filters, called elemental filters, that are run in parallel. Let $\Theta = \{\theta_j\}_{j=1}^N$ be the discrete parameter space (which can be a discretized version of a continuous space). The MMAE is then built from N elemental filters, where the jth filter is designed on the hypothesis that the true value of the parameter is θ_j. Processing the measurement at time t_k by all filters yields N versions of the innovation process at t_k:

$$r_j(k) = z(k) - H_j(k)\hat{x}_j(k \mid k-1), \qquad j = 1, 2, \ldots, N \tag{15}$$

where $z(k)$, $H_j(k)$, and $\hat{x}_j(k \mid k-1)$ are the measurement vector, the observation matrix and the a priori state estimate of the jth elemental filter at time t_k. With the innovation process of each filter, the a posteriori probability that its design hypothesis is true can be recursively computed as

$$p_j(k) = \frac{f_j(k)p_j(k-1)}{\sum_{i=1}^N f_i(k)} \tag{16}$$

where the probability density function $f_j(k)$ is

$$f_j(k) = \left\{1 \Big/ (2\pi)^{m/2}[\det \tilde{P}_j(k)]^{\frac{1}{2}}\right\} \exp\left\{-\tfrac{1}{2} r_j^T(k)\tilde{P}_j^{-1}(k)r_j(k)\right\} \tag{17}$$

the innovation process covariance is

$$\tilde{P}_j(k) = H_j(k)P_j(k \mid k-1)H_j^T(k) + R_j(k) \tag{18}$$

and $P_j(k \mid k-1)$ and $R_j(k)$ are the a priori estimation error covariance and the measurement noise covariance at time t_k, respectively. After all a posteriori probabilities have been computed, the MMAE chosen in this work then identifies the correct parameter value according to the MAP estimation principle

$$\hat{\theta}_{\text{MAP}}(k) = \arg\max_{\theta_j \in \Theta} p_j(k) \tag{19}$$

(The MMAE estimate can also be computed as a probability-weighted sum of all elemental state estimates.[14]) The basic structure of the MMAE is shown in Fig. 4.

B. Elemental Filter Design

As stated earlier, the assumption underlying the design of the MMAE used in this work is that the strategy space of the evader consists of a finite set of evasion strategies. Thus, the MMAE is built on a finite set of elemental filters, each one corresponding to an evasion strategy. Because, in the scenario considered, the evader strategy set consists of 45 elements, in theory the MMAE should have consisted of 45 elemental filters. However, to reduce the computational burden associated with the MMAE, an iterative trial-and-error process was used to select and design a six-filter MMAE, suitable for the scenario, that was found to provide an adequate performance in most cases. The elemental filters are described in Table 1.

Each elemental filter is designed using the standard EKF equations and is properly tuned to its corresponding evasion strategy. The EKF internal dynamic model comprises 1) the nonlinear equations describing the motion of the evading aircraft relative to the reference coordinate system [Eqs. (1)] and 2) two second-order shaping filters used to model the periodic evasion maneuver and the periodic EJ, that are based on the first terms of a Fourier expansion of the periodic function associated with the maneuver/jinking.[15,16] Designed to yield correct second-order statistics of the associated stochastic processes, the structure of both shaping filters, for the maneuver and the EJ, is shown in Figs. 5 and 6, respectively. In Figs. 5 and 6, u_m and u_j are white driving processes with intensities

$$q_m = \frac{64\phi^2_{e\max} L_m^2}{\pi^4 t_r^2 t_f} \tag{20}$$

Table 1 MMAE elemental filters

Filter no.	ω_m, rad/s	ω_j, rad/s	Corresponding evasion strategies
1	0.5	NJ	Most maneuver options, no EJ
2	0	1	Constant maneuver, arbitrary EJ
3	0.75	2	Periodic maneuver with $\psi_m = 0$, arbitrary EJ
4	0.75	2	Periodic maneuver with $\psi_m = \pi$, arbitrary EJ
5	0.5	0	Periodic maneuver, constant EJ with $\psi_j = 0$
6	0.5	0	Periodic maneuver, constant EJ with $\psi_j = \pi$

and

$$q_j = \frac{16W^2_{\max}}{\pi^4 t_f} \tag{21}$$

respectively, where $L_m = \pi/\omega_m$ and $L_j = \pi/\omega_j$. Here, θ_1 and θ_2 are the maneuver shaping filter states and y_{j1} and y_{j2} are the EJ shaping filter states.

The filter's augmented state vector thus obtained is

$$\boldsymbol{x} \triangleq \begin{pmatrix} z & y & \psi_e & \theta_1 & \dot\theta_1 & \theta_2 & \dot\theta_2 & y_{j1} & \dot y_{j1} & y_{j2} & \dot y_{j2} \end{pmatrix}^T \tag{22}$$

The corresponding filter's state equations are

$$\dot z = v_p \sin\theta_p \tag{23a}$$

$$\dot y = v_e \sin\psi_e - v_p \sin\psi_p \cos\theta_p \tag{23b}$$

$$\dot\psi_e = g\tan(\theta_1 + \theta_2)/v_e \tag{23c}$$

$$\ddot\theta_1 = -\theta_1 \big/ a_2^2 + (a_1/a_2)u_m \tag{23d}$$

$$\ddot\theta_2 = -9\theta_2 \big/ a_2^2 + (a_3/a_2)u_m \tag{23e}$$

$$\ddot y_{j1} = -y_{j1} \big/ b^2 + (1/b)u_j \tag{23f}$$

$$\ddot y_{j2} = -9y_{j2} \big/ b^2 + (1/b)u_j \tag{23g}$$

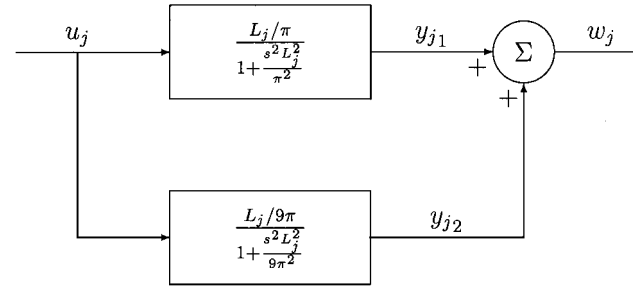

Fig. 6 EJ shaping filter.

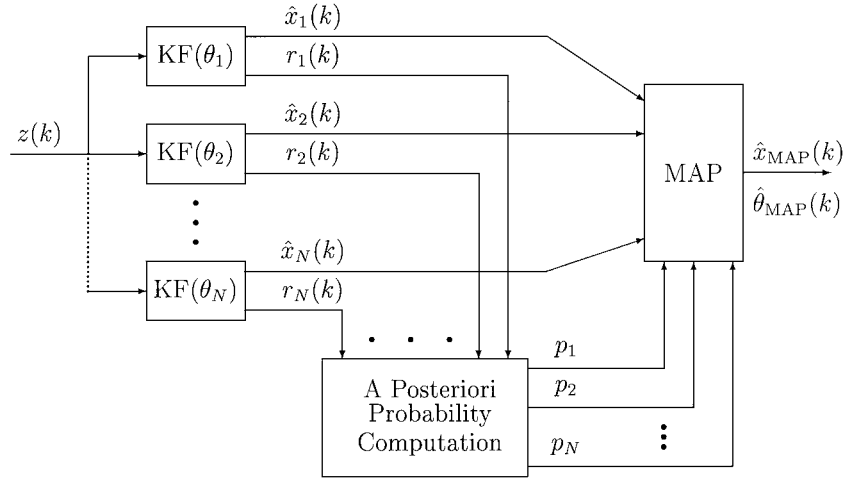

Fig. 4 Basic structure of MMAE.

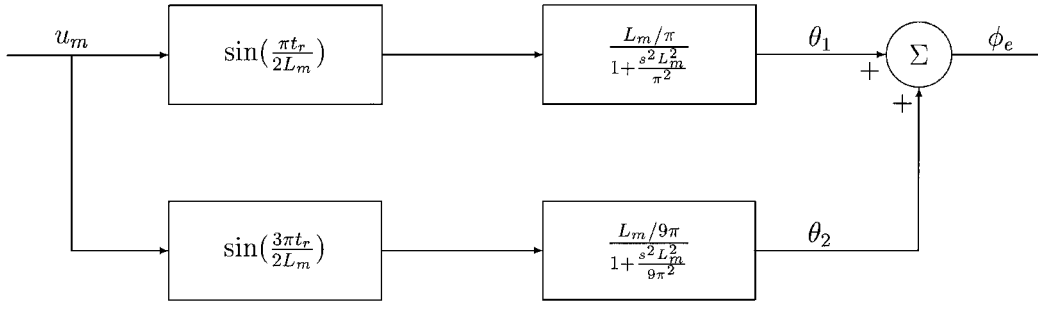

Fig. 5 Maneuver shaping filter.

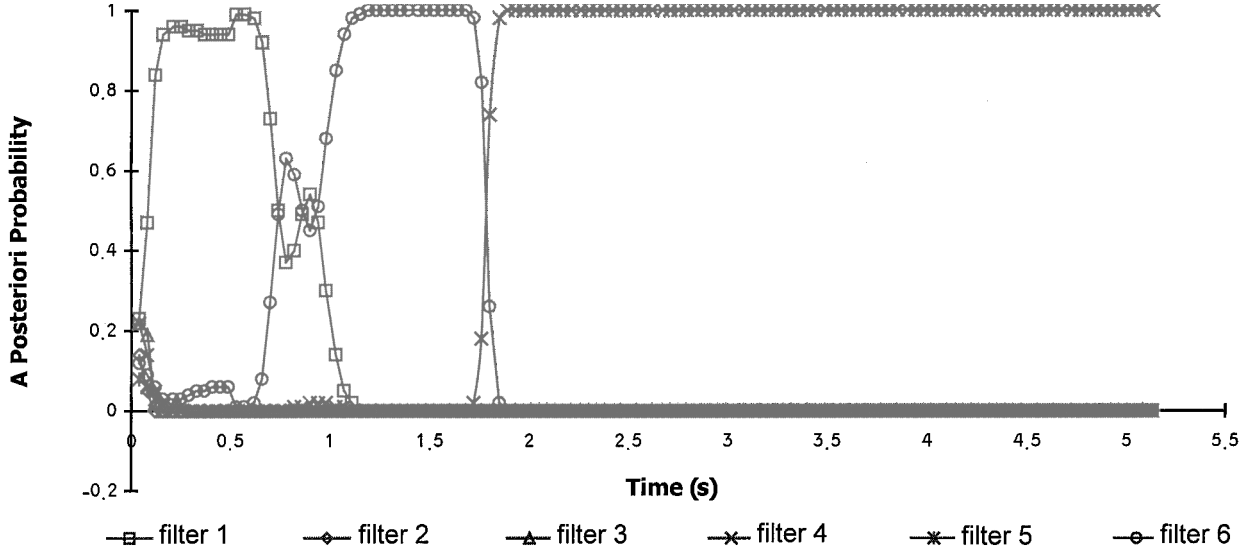

Fig. 7 Evasion strategy identification by MMAE: a posteriori probability of the elemental filters.

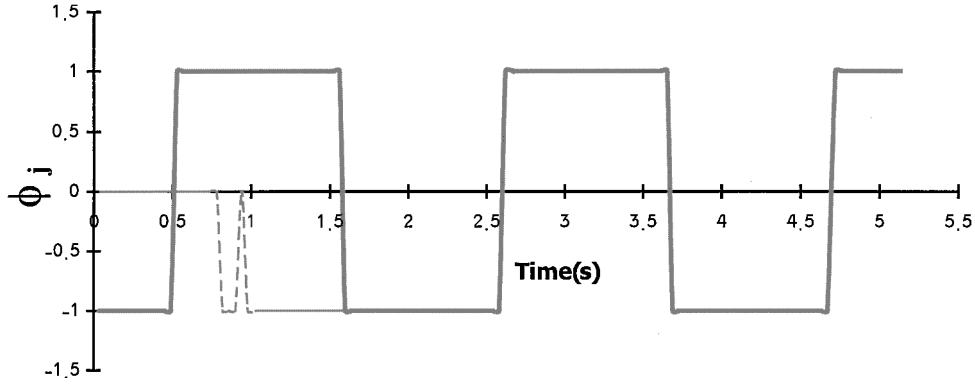

Fig. 8 Estimation performance of MMAE: EJ; ——, true, and – – –, estimate.

where the maneuver shaping filter coefficients are defined as

$$a_1 \triangleq \sin(\pi t_r/2L_m) \tag{24}$$

$$a_2 \triangleq L_m/\pi \tag{25}$$

$$a_3 \triangleq \sin(3\pi t_r/2L_m) \tag{26}$$

and the EJ shaping filter coefficient is defined as

$$b \triangleq L_j/\pi \tag{27}$$

The measurements available to the filter were described in the prceeding section. They are acquired at a rate of 25 Hz.

To properly tune the EKFs to their respective working scenarios (defined by the aircraft evasion strategies), the following modifications were implemented in the elemental filters:

1) The estimated roll angle was limited to its maximal value of $\phi_{e\max}$ (note that if this value is unknown, the assumption of a conservatively large value would lead to a smaller miss distance than that corresponding to the true value).

2) The absolute value of the estimated shift in target position due to the EJ was forced to be $W_{\max}$, with the same sign as that estimated by the filter.

3) Additional logic was introduced into the estimator to enhance its capability to distinguish between a change in the target position due to a target maneuver and a sharp change in the target center of radar reflection due to the EJ. The logic was based on the observation that changes in the target center of reflection due to EJ are discontinuous (jumps), whereas changes due to maneuver are continuous.

Figures 7–9 show the performance of the MMAE in a typical scenario where the target used EJ at a frequency of $\omega_j = 3$ rad/s and maneuvered at a frequency of $\omega_m = 0.75$ rad/s. Notice that the MMAE filter bank does not include a filter that is fully matched to this scenario. However, as can be observed from Fig. 7, which shows the a posteriori probability of the elemental filters vs time, it takes the MMAE about 2 s to identify correctly filter 4 ($\omega_j = 2$ rad/s and $\omega_m = 0.75$ rad/s) as the one that best corresponds to the scenario.

IV. Simulation Study and Discussion

The homing performance of the MMAE/DGL guided missile was tested using extensive simulations of the interception end game. The 45 different scenarios, each for a given combination of the available EM and EJ options, were repeatedly simulated either by varying the random phases of the periodical maneuvers and the EJ (216 combinations of ψ_m and ψ_j in 21 EM/EJ scenarios) or by a set of 50 Monte Carlo runs with different noise samples in the 9 NJ scenarios. In the 10 CJ/EM and CM/EJ scenarios, 72 simulations were performed with 36 different (uniformly distributed) phases both for left and right wingtip options of maneuvers. For the three NM/EJ scenarios only 36 simulations were needed. The exploration of all feasible options in the remaining scenarios required four simulations for CM/CJ and two for NM/CJ.

The parameters used for the simulation are shown in Table 2. In each simulation the miss distance and the corresponding probability of destroying the target were determined. Based on these elementary results, in each of the 45 scenarios the average miss distance, the standard deviation and the SSKP were computed. The scenarios where the average miss distance exceeded 4 m or the standard deviation exceeded 3 m were considered problematic and were singled out for further examination.

The mean values of the miss distance $\bar{R}_f$ in the analyzed scenarios are presented in Table 3.

The overall results of the extensive simulation are very encouraging. The average miss distance does not exceed 4.6 m in any scenario (see Table 3), and the guaranteed SSKP of the endgame with the parameters used in the simulations is 0.7, as can be seen from Fig. 10. Given that in this study the overall reliability of the entire guidance system was taken as $P_{d\max} = 0.9$, this can be considered an excellent result. Out of the 45 different scenarios only 10 were found to be problematic. Note, in this regard, that these scenarios were also found as worst cases in earlier studies,[2–5] where entirely different estimators were used.

One of the remarkable results is that in all of the scenarios with constant EJ (i.e., the center of radar reflection is fixed in one of the wingtips), the correct position of the center of radar reflection was identified and the missile was guided toward the aircraft's center of gravity. For a nonmaneuvering target (NM/CJ) the miss distance is only 8 cm, well within the 25 cm DZ implemented in the guidance law. Also, relatively small miss distances (much smaller than $W_{\max} = 4.7$ m) were obtained against maneuvering targets (EM/CJ).

The detailed analysis of the problematic scenarios indicates that the results of the failures (identified as miss distances larger than 4 m) can be attributed to one of the following three different reasons:

A. Failed Identification (FI)

In cases associated with this reason, the MMAE is unable to identify the scenario, which typically happens when the measurements that drive the MMAE might be associated with two (or more) similar scenarios over a substantial portion of the estimation interval. In this case, the MMAE might lock on an erroneous elemental filter (associated with one of the similar scenarios) and continue with this misidentified filter until the end of the game. Figures 11–13 show the behavior of the MMAE in a typical failed identification (FI) case. In the scenario shown, $\omega_m = 0.75$ rad/s and $\omega_j = 2$ rad/s, which correspond to filters 3 and 4. However, the MMAE locked on filter 2 ($\omega_m = 0$ rad/s and $\omega_j = 1$ rad/s) and did not change its identification until the end of the game. It was observed that if the identified and the true scenarios were identical until about 2.5 time constants before the end of the game, the MMAE would not develop a significant estimation error over the remaining short time interval, and the interception would succeed with a high probability.

Table 2 Simulation parameters

Parameter	Simulation value
Initial range	4500 m
Missile velocity	600 m/s
Aircraft velocity	300 m/s
$a_{p\max}$	150 m/s^2
$a_{e\max}$	50 m/s^2
$\phi_{e\max}$	78.7 deg
τ_p	0.2 s
T_s	1.36
t_r	2 s
$W_{\max}$	4.7 m
DZ	0.25 m

Table 3 Mean miss distances (meters)

	ω_j, rad/s				
ω_m, rad/s	NJ	0	1	2	3
NM	1.22	0.08	1.38	1.79	2.53
0	4.22	0.84	3.02	1.84	2.02
0.25	3.6	1.41	4.4	2.8	3.37
0.5	2.93	1.33	4.6	4.11	4.05
0.75	2.15	0.8	4.6	3.58	4.12
1	2.54	1.83	2.93	2.39	2.29
1.5	2.54	1.13	3.15	3.7	2.77
2	2.09	1.79	3.44	3.58	3.38
3	1.49	2.52	2.88	3.85	2.98

B. Late Identification (LI)

This case is similar to FI. The MMAE does succeed in identifying the correct scenario; however, the correct identification occurs too late for the missile guidance system to reduce the large estimation error that has developed before the correct identification. Figures 14–16 show the behavior of the MMAE in a typical late identification (LI) case. In the scenario shown, $\omega_m = 0.75$ rad/s and $\omega_j = 2$ rad/s, which correspond to filters 3 and 4. However, the MMAE locked on filter 2 ($\omega_m = 0$ rad/s and $\omega_j = 1$ rad/s) until about 0.75 s before the end of the game, when it correctly shifted to filter 3. In general, it was observed that the MMAE had to identify the correct scenario at least eight time constants before the end of the game for the guidance system to successfully intercept the target.

C. Failed Estimation (FE)

In this case, none of the six elemental filters of the MMAE is able to estimate the correct values needed for a successful interception. This can happen either because the filter bank composing the MMAE does not include a filter matched with the particular scenario, or due to a coupling between the target maneuver and the EJ,

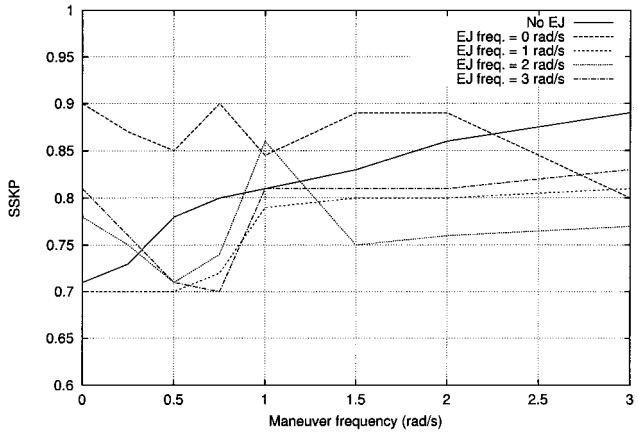

Fig. 10 SSKP for scenarios analyzed in Monte Carlo simulation.

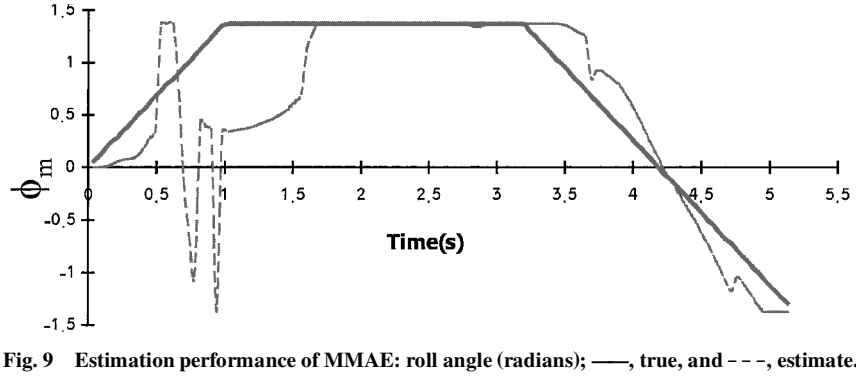

Fig. 9 Estimation performance of MMAE: roll angle (radians); ——, true, and – – –, estimate.

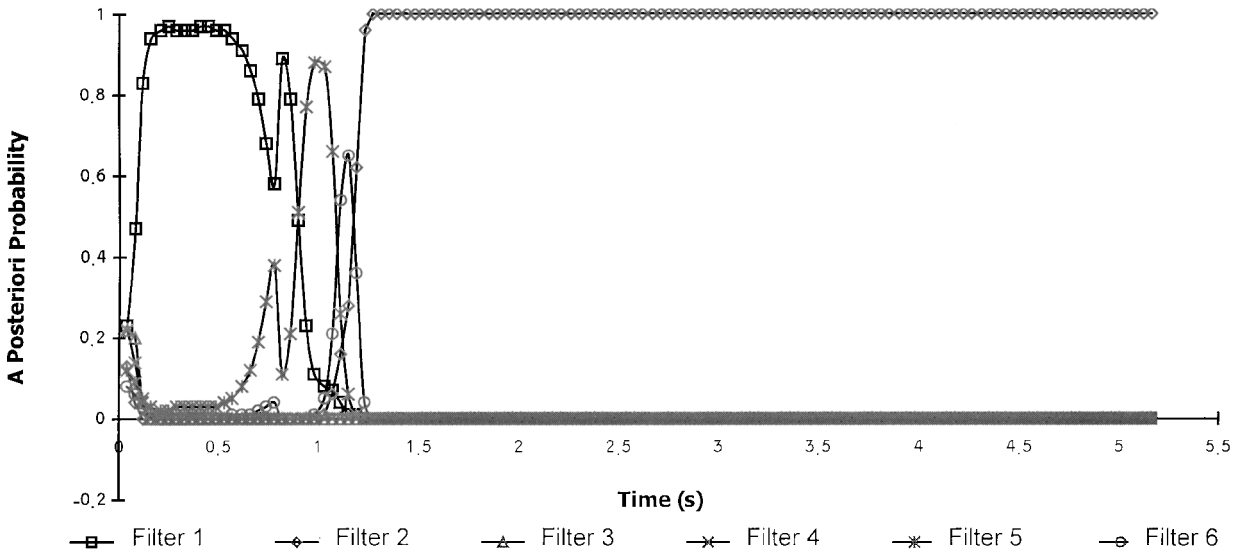

Fig. 11 Evasion strategy identification by MMAE: a posteriori probability of elemental filters in FI case.

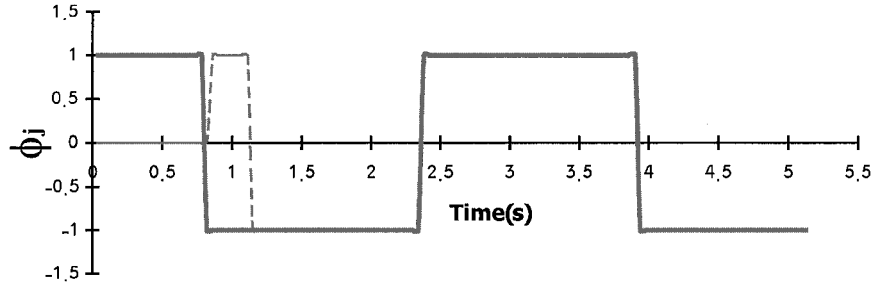

Fig. 12 Estimation performance of MMAE in FI case: EJ; ——, true, and - - -, estimate.

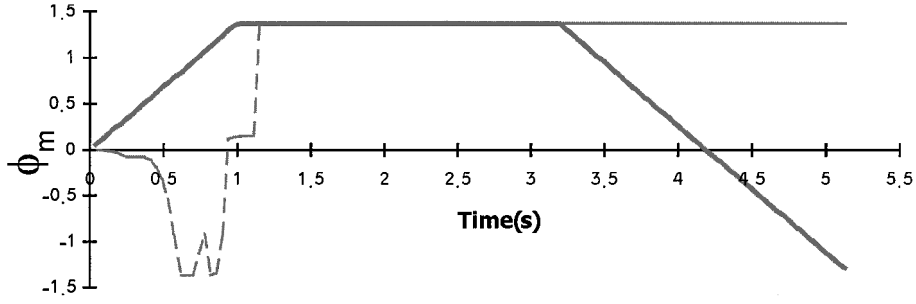

Fig. 13 Estimation performance of MMAE in FI case: roll angle (radians); ——, true, and - - -, estimate.

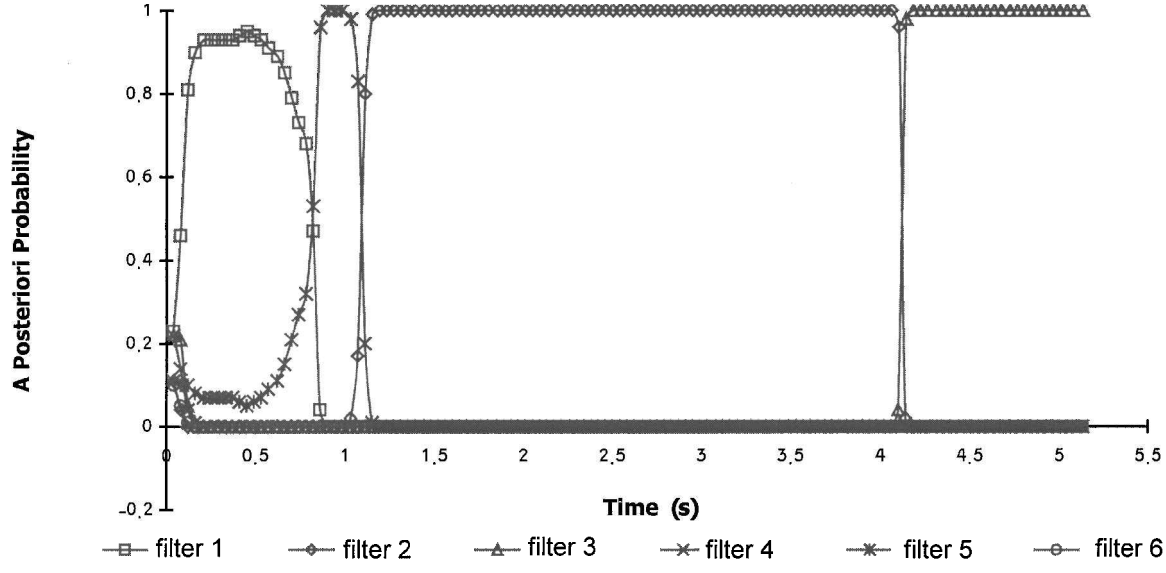

Fig. 14 Evasion strategy identification by MMAE: a posteriori probability of elemental filters in LI case.

which disturbs the roll angle estimation performance, even if the filter chosen by the bank is the filter matched with the true scenario. Figures 17–19 show the behavior of the MMAE in a typical failed estimation (FE) case. In the scenario shown, $\omega_m = 0.75$ rad/s and $\omega_j = 2$ rad/s, which correspond to filters 3 and 4. The MMAE indeed locked on filter 4, that is, correct identification; however, the maneuver/jinking coupling caused a deterioration in its estimation performance. In general, it was observed that if the deterioration due to maneuver/jinking coupling occurs more than eight time constants before the end of the game, the MMAE succeeds in recovering and the interception is successful with a high probability.

Table 4 shows the statistical distribution of these failure reasons in the simulation study performed. As can be observed from Table 4, in the six problematic scenarios examined in great detail, the average total failure rate is 23.5%. Only about 20% of all of these failures are attributed to failed or to the absence of correct scenario identification. A slightly larger percentage (24.5%) of the failures is associated with LI (less than eight time constants, that is, 1.6 s before the end of the interception). In more than half of the cases, the scenario was correctly identified, but the estimation was not sufficiently accurate. These interceptions can be characterized by a change in the maneuver direction and in the location of the center of radar reflection more or less at the same time near to the time of closest approach. Note that in most cases the switch in EJ was correctly identified almost without delay, but the estimation of the bank angle was erroneous. Figure 20 displays the coverage of the 45 end game scenarios by the filters of the MMAE. Actually, there are only four different filters because the estimators 3 and 4, as well

Table 4 Interception failure analysis

ω_m, rad/s	ω_j, rad/s	FI, %	LI, %	FE, %
0.5	1	8.8	3.2	13.4
0.5	2	3.7	5.5	12
0.5	3	2.8	6.5	17.1
0.75	1	7.9	5.1	9.3
0.75	2	3.7	4.6	12.5
0.75	3	2.3	9.7	13

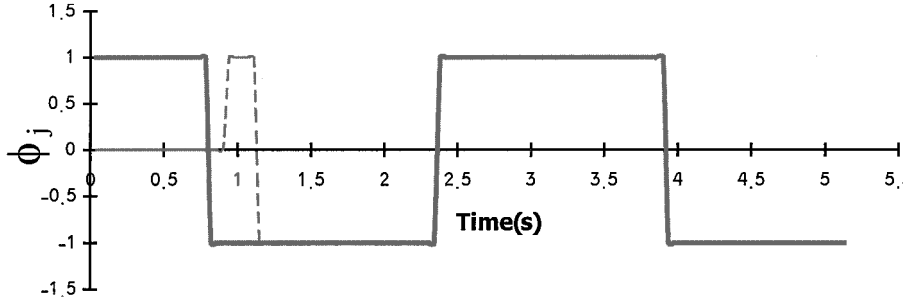

Fig. 15 Estimation performance of MMAE in LI case: EJ; ——, true, and – – –, estimate.

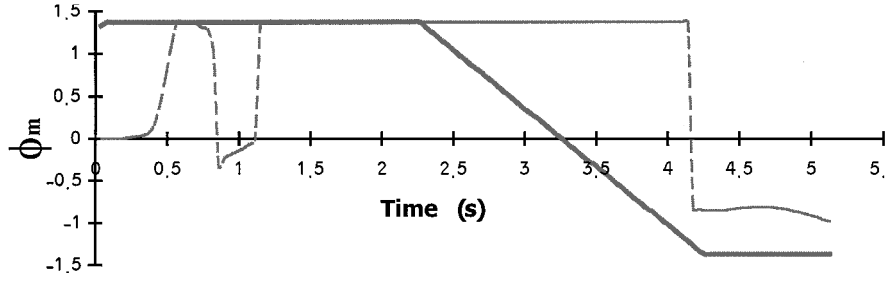

Fig. 16 Estimation performance of MMAE in LI case: roll angle (radians); ——, true, and – – –, estimate.

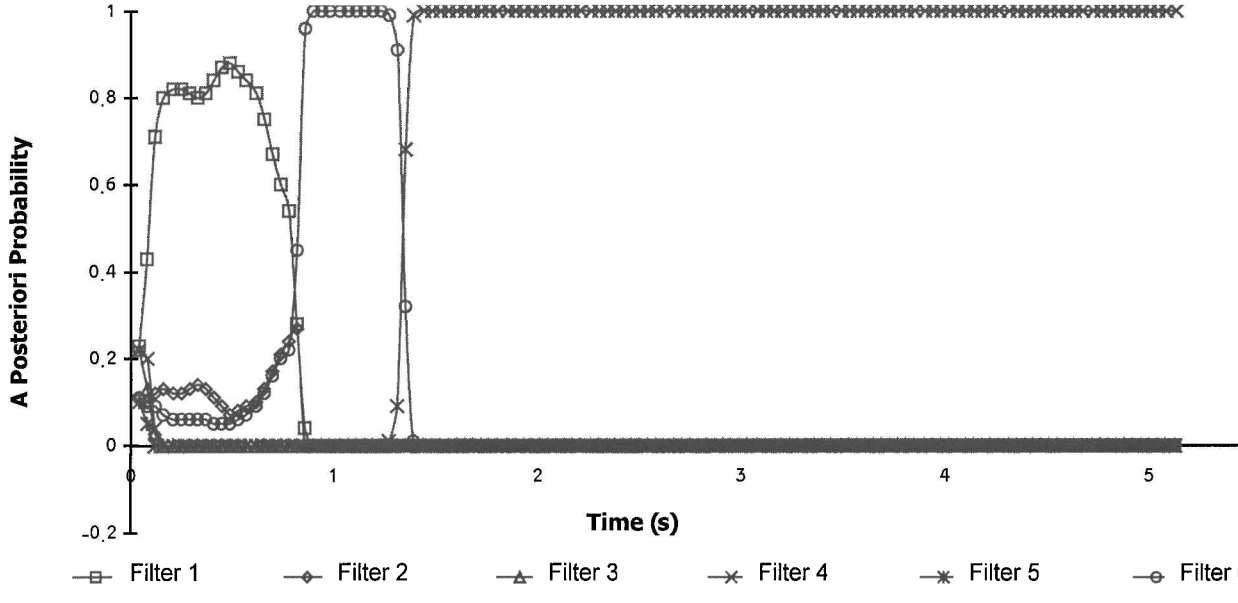

Fig. 17 Evasion strategy identification by MMAE: a posteriori probability of elemental filters in FE case.

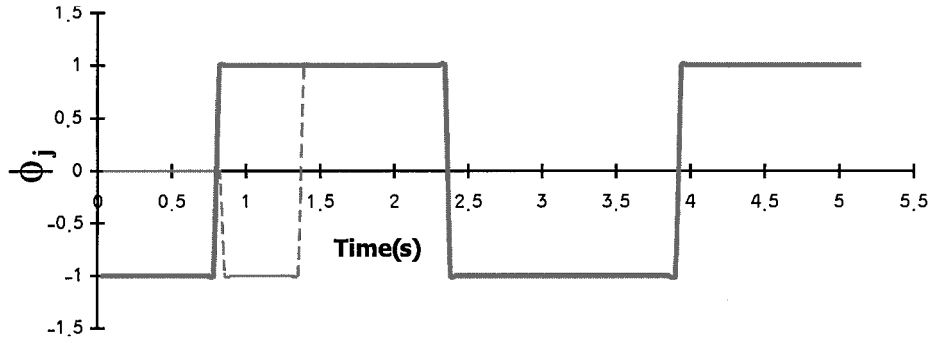

Fig. 18 Estimation performance of MMAE in FE case: EJ; ——, true, and – – –, estimate.

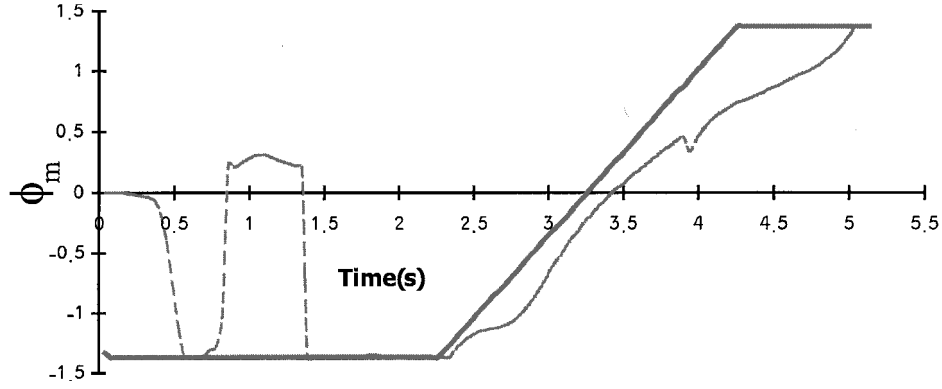

Fig. 19 Estimation performance of MMAE in FE case: roll angle (radians); ——, true, and – – –, estimate.

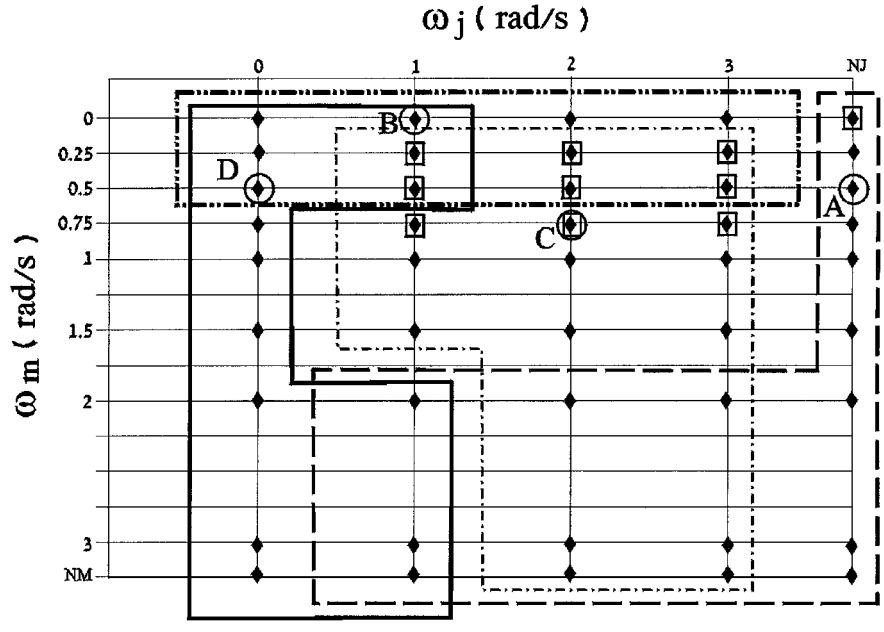

Fig. 20 Coverage of evasion strategy set by MMAE elemental filters: circles denote scenarios with matched filters in MMAE bank, squares denote problematic scenarios: – – –, filter 1, corresponding to scenario A; – – –, filter 2, corresponding to scenario B; – – –, filter 3, 4 corresponding to scenario C; and ——, filter 5, 6 corresponding to scenario D.

as 5 and 6, have identical dynamics and differ only by their assumed initial conditions. In Fig. 20, one can distinguish the four scenarios matched by the MMAE's elemental filters. The 10 problematic scenarios are also indicated. Inspection of Fig. 20 reveals that all possible evasion strategies are adequately covered by the MMAE elemental filter structure. 26 scenarios were identified to belong to (i.e., to be adequately identified by) a single elemental filter (as could be expected), 17 other scenarios were identified to belong to 2 different filters, and only 2 of the scenarios were identified to belong to 3 different filters. The identification of NJ (by estimator 1) and of CJ (by the pair 5 and 6) was performed without failure. Nonmaneuvering (NM) scenarios were also correctly identified by estimator 2. Overlapping occurred only in a part of the combined EM/EJ scenarios. In particular, it was very difficult (if not virtually impossible) to distinguish between slow maneuvering frequencies ($\omega_m = 0.25$ and 0.5) and maneuvering to a constant direction (CM)

during the short end game. In passing, note that the identification of several scenarios by more than one elemental filter, a direct consequence of the small number of filters used in the MMAE of this feasibility study, can degrade the estimator's performance in some problematic cases. When computational power allows, this problem can be adequately addressed by increasing the number of elemental filters (at the price of increasing the MMAE's complexity).

Comparison with the results published in Ref. 5 shows an impressive improvement of the guaranteed SSKP from 0.4 to 0.7 achieved by the MMAE application. When the 0.9 reliability factor is taken into account, it is essentially a decrease of 150% in the failure rate from 0.5 to 0.2. The earlier paper[5] showed that if the existence of EJ can be identified online, the guaranteed SSKP would rise from 0.4, obtained by using an optimal mixed strategy, to 0.59 for NJ and 0.65 for the EJ scenarios. Both are less than the 0.7 guaranteed by MMAE.

V. Conclusions

In this paper a new approach is presented for the design of the guidance system of an advanced air-to-air missile, equipped with an active monopulse radar seeker. The target is assumed to be a highly maneuverable aircraft also having an ECM capability. The missile's guidance system implements a guidance law based on differential game theory, obtaining the information on the relative position and velocity of the target from an MMAE. In this study the estimator comprises six elemental filters. An extensive simulation study was used to demonstrate the performance of the method and assess its effectiveness. Such a study has not yet been published, to the best of the authors' knowledge, in the open technical literature.

While representing the entire feasible domain of evasion strategies, the ensemble of 45 different interception scenarios, characterized by combinations of periodical maneuvers and EJ, was covered by only six (essentially four) estimator models of the static MMAE used in this study. Although the duration of the end game scenario is very short (about 5 s), more than 85% of the cases (from over 5800 Monte Carlo simulations) were correctly and timely identified, with an average miss distance of less than 4.6 m. These results lead to an improved homing performance expressed by a guaranteed SSKP of 0.7, which is highly superior to the guaranteed kill probability of 0.4 obtained in earlier works, where mixed strategies were used.

This study succeeded in demonstrating, within its limited scope, that application of the adaptive estimation concept can yield satisfactory results even in the very critical air-to-air interception end game, where the target aircraft can randomly select any combination of periodical maneuvering and EJ, leading to the catastrophic failure of conventional guidance methods. Although the present work did not address some additional, practical aspects of the interception problem, the study does indicate that the implementation of this concept in real time is feasible in any modern, radar-equipped, air-to-air missile using state-of-the-art computational technology. This study also provided several examples showing that correct identification is a necessary, but not always sufficient, condition to adequate estimation performance in an end game guidance process, if the critical variables change near the time of closest approach.

Note that, in spite of the impressive improvement in guaranteed homing performance, the results achieved in this study are only suboptimal. The practice of using a perfect information guidance law in a stochastic interception scenario, such as the one discussed in this paper, is based on the assumption that the stochastic guidance problem possesses the certainty equivalence property. Moreover, the use of the estimated variables, obtained from a separately designed estimator, in the guidance law is based on the assumption that the optimal guidance problem is also separable, that is, that the optimal estimation algorithm does not depend on the optimal guidance law and vice versa. Because these assumptions do not hold true for the problem analyzed in this paper, the method used herein is clearly not optimal in a rigorous sense. Nevertheless, it was suggested in the past that for such cases a separate design of the estimator is allowed, but that the optimization of the control law should be based on the probability density function of the estimated state variables. Therefore, it is anticipated that further research in this direction, as well as more sophisticated, multiple-model estimation methods will yield even better homing performance.

Acknowledgment

This work is based on the third author's M.S. research thesis in the Department of Aerospace Engineering at the Technion—Israel Institute of Technology.

References

[1]Connelly, M. E., "An Investigation of the Use of Electronic Jinking to Enhance Aircraft Survivability," Air Force Office of Scientific Research TR AFOSR-TR-81-0455, April 1981.

[2]Forte, I., and Shinar, J., "Can a Mixed Guidance Strategy Improve Missile Performance?," *Journal of Guidance, Control, and Dynamics*, Vol. 11, No. 1, 1988, pp. 53–59.

[3]Forte, I., and Shinar, J., "Improved Guidance Law Design Based on Mixed Strategy Concept," *Journal of Guidance, Control, and Dynamics*, Vol. 12, No. 5, 1989, pp. 739–745.

[4]Shinar, J., and Forte, I., "On the Optimal Pure Strategy Sets for a Mixed Missile Guidance Law Synthesis," *IEEE Transactions on Automatic Control*, Vol. AC-36, No. 11, 1991, pp. 1296–1300.

[5]Shinar, J., Forte, I., and Kantor, B., "Mixed Strategy Guidance: A New High-Performance Missile Guidance Law," *Journal of Guidance, Control, and Dynamics*, Vol. 16, No. 1, 1994, pp. 129–135.

[6]Gutman, S., "On Optimal Guidance for Homing Missiles," *Journal of Guidance and Control*, Vol. 2, No. 4, 1979, pp. 296–300.

[7]Shinar, J., and Gutman, S., "Three Dimensional Optimal Pursuit and Evasion With Bounded Controls," *IEEE Transactions on Automatic Control*, Vol. AC-25, No. 3, 1980, pp. 492–496.

[8]Anderson, G. M., "Comparison of Optimal Control and Differential Game Intercept Missile Guidance Laws," *Journal of Guidance, Control, and Dynamics*, Vol. 4, No. 2, 1981, pp. 109–115.

[9]Zarchan, P., *Tactical and Strategic Missile Guidance*, AIAA, Washington, DC, 1990, pp. 87–110, 155–175.

[10]Chang, C. B., and Tabaczynski, J. A., "Application of State Estimation to Target Tracking," *IEEE Transactions on Automatic Control*, Vol. AC-29, No. 2, 1984, pp. 98–109.

[11]Singer, R. A., "Estimating Optimal Tracking Filter Performance for Manned Maneuvering Targets," *IEEE Transactions on Aerospace and Electronic Systems*, Vol. AES-6, No. 4, 1970, pp. 473–483.

[12]Speyer, J. L., Kim, K. D., and Tahk, M., "Passive Homing Missile Guidance Law Based on New Target Maneuver Models," *Journal of Guidance, Control, and Dynamics*, Vol. 13, No. 5, 1990, pp. 803–812.

[13]Bowman, G. A., and Speyer, J. L., "Detection Filters for Missile Tracking," *Proceedings of the AIAA Guidance, Navigation, and Control Conference*, AIAA, New York, 1987, pp. 570–578.

[14]Maybeck, P. S., *Stochastic Models, Estimation and Control*, Vol. 2, Academic, New York, 1982, Chap. 10, p. 129.

[15]Zarchan, P., "Representation of Realistic Evasive Maneuvers by the Use of Shaping Filters," *Journal of Guidance and Control*, Vol. 2, No. 4, 1979, pp. 290–295.

[16]Fitzgerald, R. J., "Shaping Filters for Disturbances with Random Starting Times," *Journal of Guidance and Control*, Vol. 2, No. 2, 1979, pp. 152–154.